Malaria Journal

RESEARCH

Open Access

In vitro and in silico evaluation of synthetic compounds derived from bi-triazoles against asexual and sexual forms of *Plasmodium falciparum*

Leandro do Nascimento Martinez[1,2,3*], Minelly Azevedo da Silva[4,5], Saara Neri Fialho[1,3,5], Marcinete Latorre Almeida[1,5], Amália dos Santos Ferreira[1], Aurileya de Jesus Gouveia[1], Welington da Silva Paula do Nascimento[1,5], Ana Paula de Azevedo dos Santos[3], Norton Rubens Diunior Lucas Pejara Rossi[1], Jansen Fernandes de Medeiros[2,6,8], Natalie Ferreira Araújo[7], Quelli Larissa Oliveira de Santana[7], Carlos Roland Kaiser[7], Sabrina Baptista Ferreira[7], Maisa da Silva Araujo[5,6,8] and Carolina Bioni Garcia Teles[1,2,3,5,8]

Abstract

Background Despite advances in malaria chemotherapy, the disease continues to claim thousands of lives annually. Addressing this issue requires the discovery of new compounds to counteract resistance threatening the current therapeutic arsenal. In this context, bi-triazoles are substances with diverse biological activities, showing promise as lead compound to fight malaria. Triazoles are heterocyclic structures composed of five members, including three nitrogen atoms and two double bonds. Bi-triazoles, the focus of this study, are derivatives of triazoles consisting of two triazole rings (nitrogen heterocyclic) with isolated nuclei lacking a spacer and two substituents at each end. The goal of the present study was to assess the in vitro and in silico, antimalarial activity of bi-triazole compounds 14c, 14d, 13c, and 13d against asexual and sexual forms of *Plasmodium falciparum*.

Methods For in silico predictions, the software OSIRIS, Molinspiration, and ADMETlab were employed. To determine the 50% inhibitory concentration (IC_{50}) on the asexual forms, the W2 clone was used, while the strain NF54 was used to assess inhibition of sexual forms. Cytotoxicity was evaluated using the HepG2 cell line, and haemolysis tests were conducted. Additionally, the selectivity index (SI) of each compound was calculated.

Results In silico analyses of physicochemical properties revealed that all compounds have favorable potential for drug development. Pharmacokinetics predictions also provided important, novel insights into this chemical class. Antimalarial activity tests showed that compounds 14d and 13d exhibited promising activity, with IC_{50} values of 3.1 and 4.4 µM, respectively. Antimalarial activity of compounds 14d and 13d may be related to the presence of methyl acetate in substituent R_2 conjugated to the bi-triazole. None of the compounds demonstrated cytotoxic or haemolytic activity, with SI values above 51 for the three most active compounds, highlighting their selectivity. For the sexual forms, compounds 14c and 14d were classified as having a high potential to block malaria transmission.

*Correspondence:
Leandro do Nascimento Martinez
leandro.martinez@fiocruz.br
Full list of author information is available at the end of the article

Conclusion Overall, the in vitro and in silico results showed that bi-triazole compounds may guide new biological investigation for malaria, enabling the identification and development of more active and selective antimalarial agents.

Keywords Bi-triazoles, Gametocytes, Transmission blocking, *Plasmodium falciparum*, In silico

Background

Despite recent advances in public health, malaria remains a leading causes of death worldwide. Data from the World Health Organization (WHO) indicate that between 2000 and 2022, the total mortality caused by malaria decreased by 30%, although new cases increased by 2.4% during the same period. This significant reduction in mortality reflects progress in malarial control efforts across endemic regions. However, the increase in new cases is intrinsically related to the COVID-19 pandemic, which exacerbated political and social instability in many countries [1].

Over time, resistance to antimalarial drugs has been observed in *Plasmodium falciparum* and *Plasmodium vivax* around the world [2, 3]. Notably, resistance of *P. falciparum* to artemisinin derivatives has been reported in Southeast Asia [4], posing a major threat to malaria control efforts. In this scenario, there is an urgent need for new chemical compounds target multi-stage of the parasite's lifecycle, including as asexual erythrocytic, hepatic, sexual, and sporogonic stages, to function as multi-stage antimalarials [5]. The parasite's complex lifecycle, involving both invertebrate and vertebrate hosts and encompassing asexual and sexual stages, complicates the development of effective treatments [6].

The current arsenal of antimalarial drugs is limited, which varying efficacy against asexual and sexual stages of the parasite [7]. Artemisinin-based compounds effectively target asexual erythrocytic stages (rings, mature trophozoites, and schizonts) and early gametocyte stages (I–III), but their efficacy against mature stage V gametocytes is limited [8]. Consequently, artemisinins alone do not completely prevent post-treatment transmission. Currently, primaquine is the only approved compound for gametocyte elimination [9]. However, its use is limited by serious side effects, including acute haemolytic anaemia in individuals with glucose-6-phosphate dehydrogenase (G6PD) deficiency, and contraindications in pregnant women and young infants [10]. WHO guidelines recommend a low dose of primaquine (0.25 kg/mg) for the eliminate mature *P. falciparum* gametocytes, which minimizes the risk of causing haemolysis in G6PD-deficient individuals [11]. Primaquine is also used to prevent relapses in *P. vivax* and *Plasmodium ovale* infections, through with some limitations [12]. Therefore, it is essential to seek new compounds that block malaria transmission. Some authors point out that, for countries that are already in the advanced phase of malaria elimination, the fight against this pathology should include the elimination of gametocytes from the host to prevent transmission to malaria vectors [13, 14]. This approach represents a critical step in the broader goal of eliminating malaria.

The diverse biological activities of bi-triazoles, such as antiviral [15], antibacterial [16], and antiplasmodial [17] properties, make this chemical class, derived from triazoles, a promising candidate for the development of molecules with potential antiplasmodial activity. The limited number of studies on bi-triazoles further underscores the importance of exploring this chemical class for antiplasmodial applications.

In the rational screening of potential antimalarial candidates, various software tools have been developed to facilitate in virtual (in silico) screening of molecules. These tools enable the modelling of pharmacokinetic, pharmacodynamic (mechanism of action), and physicochemical properties, providing valuable insights. The results from such screenings can guide improvements in the bioactivity of molecules in subsequent in vitro and in vivo experiments, reducing research costs and optimizing time in the selection of a potential drug candidates [18].

This study aims to determine the physicochemical and pharmacokinetic properties of bi-triazoles through in silico tests and identify new compounds with blood schizontocidal and gametocytocidal activity against *P. falciparum*.

Methods

Compound synthesis

The synthesis of bi-triazole was reported by Addla et al. [17], with the methodology described in their study. The synthetic route begins with the preparation of amino triazoles (10a and 10b) as starting materials (Fig. 1). The synthesis of 2-amino-1,2,4-1H-triazoles substituted at position 5 involves the condensation and cyclization of aminoguanidine bicarbonate (1) with acetic or trifluoroacetic acids. Subsequently, azides (3a and 3b) were synthesized via a diazotization reaction. The desired bi-triazoles were then obtained through a Huisgen 1,3-dipolar cycloaddition reaction between the azide derivatives and commercially available terminal

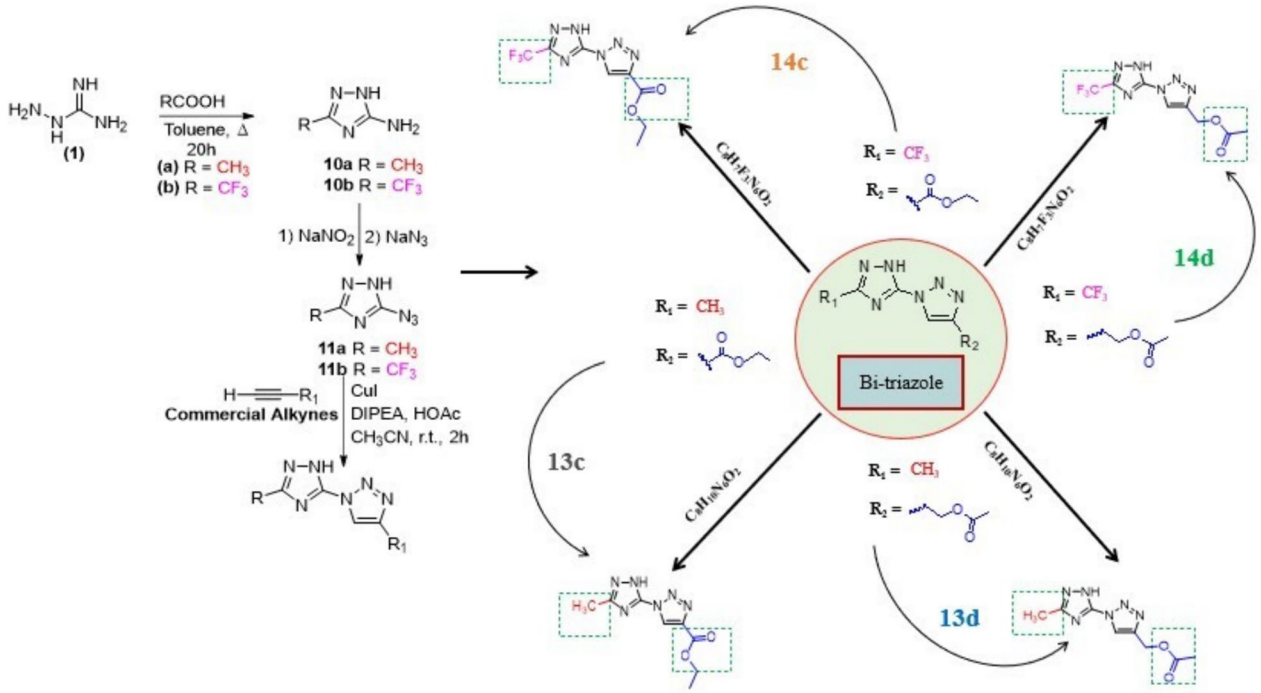

Fig. 1 Synthesis of substituted bi-triazoles. Structure of bi-triazoles derived from 1,2,3-triazoles by conventional heating (10a; 10b; 11a and 11b). Structure of bi-triazole compounds 1-(3-(trifluoromethyl)-1H-1,2,4-triazol-5-yl)-1H-1,2,3-triazole-4-carboxylate (14c); (1-(5-(trifluoromethyl)-1H-1,2,4-triazol-3-yl)-1H-1,2,3-triazol-4-yl)methyl acetate (14d); 1-(3-methyl-1H-1,2,4-triazol-5-yl)-1H-1,2,3-triazole-4-carboxylate (13c); (1-(5-methyl-1H-1,2,4-triazol-3-yl)-1H-1,2,3-triazol-4-yl)methyl acetate (13d), showing the insertion of the respective R1 and R2 radicals through click chemistry synthesis. *CuI* Copper(I) iodide, *DIPEA* N,N-Diisopropylethylamine, *HOAc* Acetic acid

alkynes. This reaction was catalyzed by Cu(I) in the presence of diisopropylethylamine, acetonitrile, and acetic acid. The formation of triazole required the presence of Cu(I) as a catalyst. In the initial step of the mechanism, Cu(I) facilitates π complexation with the terminal alkyne, reducing the pKa of the alkyne and enabling its deprotonation without the need for a strong base. This step leads to the formation of copper acetylide, which subsequently forms a complex with azide. The copper catalyst enhances the electrophilicity of the azide's terminal nitrogen and the nucleophilicity of the β-vinylidene carbon, promoting the formation of a metallocycle. This metallocycle ultimately generates copper triazolyl, which undergoes protonation to yield the final bi-triazole products, as reported by Addla et al. [17].

The bi-triazole compounds were solubilized in dimethyl sulfoxide (DMSO) (Sigma-Aldrich), with a maximum concentration of 0.5%, as higher concentrations are known to be toxic to the parasite [19]. For the cytotoxicity assays, the maximum DMSO concentration was set at 1%, as higher levels are considered toxic to cell lines [20]. The compounds were tested in two or three independent experiments, each performed in triplicate.

In silico prediction

OSIRIS

The solubility (LogS) of the compounds was predicted using OSIRIS platform to assess their solubility in aqueous medium. The classification parameters for the LogS value were as follows: insoluble (≤ -10); slightly soluble (≤ -6); moderately soluble (≤ -4); soluble (≤ -2), and highly soluble (≤ 0) [21]. Additional parameters, including drug score and drug-likeness, were also predicted. These values are widely used in the selection of new compounds with potential pharmaceuticals applications. Drug-likeness values can be either as positive or negative, with positive values indicating that the compound shares similarities with commercially available drugs, while negative values indicate the opposite. Drug score values range from 0 to 1, with values closer to 1 indicating that the compound has a higher likelihood of qualifying as a pharmaceutical agent. The drug score is derived from the compound's physicochemical characteristics, toxicity alerts, and drug-likeness score (https://www.organic-chemistry.org/prog/peo/). The OSIRIS Property Explorer database includes approximately 5300 compounds. These compounds are composed of fragments derived from 3.300 commercial available pharmaceuticals and 15,000

chemicals sourced from Fluka (Charlotte, North Carolina, EUA).

Molinspiration

The Molinspiration platform (http://www.molinspiration.com) was used to predict and evaluate key physicochemical parameters, including polar surface area (PSA), hydrogen bond acceptors (HBA), hydrogen bond donors (HBD), number of violations (VIO), number of rotatable bonds (ROT) and molecular volume (VOL). The software uses the number of violations (compounds with values exceeding 1 may present challenges in oral bioavailability) and Lipinski's Rule of Five to classify compounds as possible drug candidates. To qualify, molecule must satisfy the following criterial: logP ≤ 5, molecular mass ≤ 500 g/mol, HBA ≤ 10 (expressed as the sum of nitrogen (N) and oxygen (O) atoms), and HBD ≤ 5 (calculated as the sum of OH and NH groups) [22]. Additional parameters considered in this study included PSA ≤ 140 Å and ROT ≤ 10, as both are related to oral bioavailability, according to Veber et al. [23].

ADMETlab

The ADMETlab platform (http://admet.scbdd.com/), was employed for an in silico assessment of physicochemical properties, including lipophilicity (LogP), absorption (Caco-2 cell permeability, Pgp inhibition, and Pgp substrate activity), distribution (plasma protein binding-PPB); volume of distribution (Vd), and blood–brain barrier (BBB), metabolism (inhibition of cytochrome P450 inhibitor: CYP1A, CYP3A4, CYP2C9, CYP2C19, and CYP2D6), and elimination (half-life-T ½) and clearance—CL). Additionally, the platform evaluated toxicity parameters such as LD_{50} (dose to kill 50% of the population), drug-induced liver injury (DILI), FDA maximum recommended daily dose (FDAMDD), and hERG (ether-a-go-go-related gene) channel blockade.

The ADMETlab database, comprising 288,976 entries, supports systematic evaluations. For the in silico prediction of cLogP, the following classifications were used: (i) values between 0 and 3 indicate are moderate properties, balancing permeability and solubility; values ≤ 0 means low permeability of the lipid bilayer (hydrophilic molecules), (iii) values ≥ 3 means low solubility in aqueous medium (hydrophobic molecules) [24]. For Caco-2 cell permeability (log Papp), the following thresholds were applied, as described by Pham The et al. [25]: ≥ log $(8 \times 10^{-6}) = -5.09$: high solubility; ≤ log $(8 \times 10^{-6}) = -4.69$ to -5.09: moderate solubility; ≤ log $(20 \times 10^{-6}) = -4.69$: low solubility. For Pgp inhibitors and substrates, positive and negative values were recorded to indicate activity or inactivity, respectively [26, 27].

For plasma protein binding (PPB), values above 75% are considered HPPB (compounds with high PPB, or class 1) and values ≤ 75% are considered LPPB (compounds with low PPB, or class 0) [28]. Regarding the volume of distribution (Vd), a range from 0.04 L/kg^1 to 20 L/kg^1 was considered, corresponding to approximately 2.8 to 1400 L for an individual weighing 70 kg [29]. Blood–brain barrier (BBB) penetration was evaluated, with positive values indicating the ability to cross the BBB and negative values indicating non-penetration [30]. Compounds classified as hERG-blockers were categorized as either positive or negative, according to Sanguinetti et al. [31].

For P450 enzymes (CYP), values were recorded either positive or negative. Drug half-life (T ½) was categorized as follows: low (≤ 3 h); long (≥ 8 h); and moderate (between 3 and 8 h) [32]. Clearance (CL) was classified as high (≥ 15 mL/min/kg); moderate (between 15 mL/min/kg and 5 mL/min/kg); and low (≤ 5 mL/min/kg) [32]. LD_{50} values were grouped into six toxicity classes based on their lethal dose: class I-Lethal ($LD_{50} \leq 5$ mg/kg); class II: Lethal (5 mg/kg ≤ LD_{50} ≤ 50 mg/kg); class III: Toxic (50 mg/kg ≤ LD_{50} ≤ 300 mg/kg); class IV: Harmful (300 mg/kg ≤ LD_{50} ≤ 2,000 mg/kg); class V: may be harmful (2,000 mg/kg ≤ LD_{50} ≤ 5,000 mg/kg); class VI: Non-toxic ($LD_{50} \geq 5{,}000$ mg/kg) [33]. Drug-induced liver injury (DILI) and FDA maximum recommended daily dose (FDAMDD) were categorized as positive or negative, according to their respective parameters [34, 35].

Biological activity

In vitro culture of Plasmodium falciparum

The *P. falciparum* W2 and NF54 strains were cultured in human O^+ red blood cells using 10.4 g/L RPMI 1640 medium (Gibco) supplemented with 25 mM HEPES (Sigma-Aldrich), 0.3 mM hypoxanthine (Sigma-Aldrich), 23.80 mM sodium bicarbonate (Sigma-Aldrich), 40 mg/L gentamicin (NOVAFRMA), and either 10% (v/v) O^+ human plasma or 2.5 mg/L (v/v 5%) Albumax II (Gibco), following the conditions established by Trager and Jensen [36]. Cultures were initiated at a haematocrit of 5% and maintained in an incubator at 37 °C under a gas mixture containing 5% CO_2, 5% O_2, and 90% N_2. Medium were changed every 48 h.

Parasitaemia was monitored using thin smears stained with a panoptic kit (Newprov) and examined under an optical microscope (NIKON L 200) at 1000 × magnification. Parasitaemia development stages were observed by analysing 1000 red blood cells. When parasitaemia exceeded 8% young trophozoites, cultures were synchronized with 5% sorbitol [37]. The 50% inhibitory concentration (IC_{50}) value were determined using the SYBR Green I assay.

In vitro antimalarial activity assessment via the SYBR Green I assay against the P. falciparum W2 clone

Following synchronization of the *P. falciparum* W2 Indochina clone culture, 180 µL/well of culture containing 0.5% parasitaemia and 2% haematocrit was distributed into 96-well microplates U-bottom microplates (OLEN). Compounds 14c, 14d, 13c and 13d were added in triplicate, with 20 µL of each compound prepared in a 1:2 serial dilution, resulting in a final concentration ranging from 1.56 to 200 µM. Artemisinin (Art) at a final concentration of 170 nM was used as positive control. Positive growth controls infected red blood cells infected without treatment, and non-infected red blood cells were used as blanks, with their fluorescence subtracted from observed values.

The experimental cultures were incubated at 37 °C under a gaseous mixture (5% CO_2, 5% O_2, and 90% N_2) for 72 h. At the end of the incubation period, the supernatant was removed without disturbing the red cell pellets. Subsequently, 100 µL of phosphate-buffered saline (1 × PBS) were added to each well, and the plates were centrifuged at 478 × *g* for 10 min.

After centrifugation, the supernatant was removed, and 100 µL of lysis buffer (20 mM Tris–HCl (Sigma-Aldrich), 5 mM EDTA (Sigma-Aldrich), 0.008% saponin (Sigma-Aldrich), 0.08% Triton X-100 (GE Healthcare) containing 0.02 µL SYBR Green I at 10,000 × concentration (Invitrogen) were added. The solution was homogenized, and 100 µL were transferred to a flat-bottom microplate (KASVI) containing 100 µL PBS 1x. The plates were incubated for 30 min at 24 °C, protected from light. Fluorescence was measured using a multi-detection system (BioTek Synergy HT) with an excitation wavelength of 485 nm and an emission wavelength of 590 nm, using a gain of 100 [38, 39]. Compounds with IC_{50} values ≤ 25 µM were considered as active [40].

Cytotoxic activity evaluation via the MTT method

To determine the cytotoxic concentration (CC_{50}) that affects 50% of the cell population, the human hepatocellular carcinoma cell line (HepG2) was used. Cells were cultured following the protocol established by Calvo-Calle et al. [41]. They were cultivated in 25 cm^2 culture flasks with Techno Plastic Products (TPP) filter, using RPMI 1640 medium (Gibco) supplemented with 10% (v/v) bovine fetal serum (BFS, Gibco) and 40 mg/L gentamicin. Cultures were incubated at 37 °C with 95% humidity and 5% CO_2 to promote adherence. Cells were seeded every three days.

Once the cultures reached approximately 90% confluence, cells were trypsinized using a solution containing 0.05% trypsin (Sigma-Aldrich) and 0.5 mM EDTA (Dinâmica). For the cell adherence step, cells were adjusted to a concentration of 1×10^4/mL cells/well and in plated in 96-well microplates (KASVI) with 180 µL/well of RPMI 1640 medium supplemented with 10% (v/v) BFS (Gibco) and 40 mg/L gentamicin. The paltes were incubated in a 5% CO_2 at 37 °C for 72 h [41]. All compounds were tested at serial concentrations starting from a final concentration of 500 to 0.244 µM.

The compounds were independently tested in triplicate, with at least two repetitions. Non-treated cells were employed as viability control, cells treated with lysis buffer were used as positive control, and RPMI 1640 medium was used as blank. Plates were incubated for 72 h. Four hours before the end of the incubation, 20 µL of a 3-[4,5-dimethylthiazol-2-yl]-2,5 diphenyl tetrazolium bromide (MTT) solution (5 mg/mL in PBS 1x) were added to each well [42]. At the end of the incubation period, the supernatant was discarded, and 100 µL/well DMSO were added to solubilize the formazan crystals produced by metabolically active cells.

Absorbance was measured at 570 nm using a spectrophotometer (Biochrom Asys Expert Plus) with a blank absorbance subtracted from the measured values.

Haemolysis assay

The compounds were diluted in plates under the same conditions and concentration described in Sect. 2.4.2. Subsequently, 20 µL of the test compounds were added to a 1% red blood cell suspension (180 µL) in a 96-well U-bottom plate (KASVI). The bi-triazole compounds were diluted to final concentrations ranging from 200 to 1.56 µM.

A 0.05% saponin solution was used as positive control, while untreated red blood cells were used as negative control. RPMI 1640 medium was used as blank to subtract background absorbance from all samples. The plate was incubated at 37 °C for 30 min with periodic stirring every 5 min. After incubation, the plate was centrifuged at 478 *g* for 10 min, and the supernatant was transferred to a flat-bottom plate [43]. Absorbance was measured at a wavelength of 540 nm using the Biochrom Asys Expert Plus spectrophotometer. Results were expressed as optical density (OD).

Determination of the selectivity index

The selectivity index (SI) was calculated by dividing the CC_{50} by the IC_{50} values. Substances with SI values ≥ 10 were classified as selective, while those with values below 10 were classified non-selective toward parasites [44–46].

In vitro tests with P. falciparum gametocytes

The NF54 strain was used for gametocyte induction according to the protocol established Delves et al. [47]. After observing the predominance of immature

trophozoites, the cultures were synchronized (day 0) [37]. Parasitaemia was adjusted to 2%, and haematocrit to 5%, in a final volume of 5 mL RMPI 1640 culture medium (Gibco) supplemented with 25 mM HEPES (Sigma-Aldrich), 50 mg/L hypoxanthine (Sigma-Aldrich), 23.80 mM sodium bicarbonate (Sigma-Aldrich), 40 mg/mL gentamicin sulfate, 10% (v/v) O^+ human serum, and 2.5 mg/L Albumax II (Gibco) under conditions established adapted from Delves et al. [47] and Duffy and Avery [48] with some modifications.

The culture medium was replaced daily after pre-heating at 37 °C. At the moment of replacement, all culture bottles were stored in an incubator (Êxodo Científica) at 37 °C. Parasitaemia was monitored using thin blood smears stained with a panoptic kit. Follow-up was performed from days 2 to 16 [47] by counting 5000 red blood cells and differentiating between asexual stage and immature and mature gametocyte stages (I–V). When parasitaemia reached ≥ 2% gametocytes in the early stages (I, II), the culture was treated daily for four consecutive days with 20 U/mL heparin (HEMOFOL) to eliminate residual asexual forms from the culture [49].

Exflagellation induction

The exflagellation procedure was initiated when parasitaemia of mature micro- and macrogametocytes (IV, V) exceeded 0.4%. The highest percentage of mature gametocytes was observed between the 12 and 16 days post-induction.

Exflagellation was induced according to the protocol by Leba et al. [50] and Delves et al. 2013 [14] with modifications. Briefly, 200 µL of culture were transferred to a 1.5 mL tube pre-heated to 37 °C and centrifuged at 637 g for 30 s at room temperature (24 °C). The supernatant was discarded, and the cell pellet was resuspended in 20 µL of ookinete medium (10.4 g/L RPMI 1640—Gibco) supplemented with 25 mM HEPES (Sigma-Aldrich), 0.36 mM hypoxanthine (Sigma-Aldrich), 23.80 mM sodium bicarbonate (Sigma-Aldrich), and 100 mM xanthurenic acid (Sigma-Aldrich), pre-heated to 37 °C [47].

The parasites, suspended in ookinete medium, were incubated for 20 min at 24 °C in a BOD (biochemical oxygen demand) incubator. After incubation, 3 µL of the culture were placed on a slide (OLEN) and covered with a 0.13–0.16 mm thick cover slip (GLASSCYTO) for microscopic examination. Exflagellation was observed under a NIKON ECLIPSE E200 optical microscope at 1000 × magnification. The exflagellation count was determined by examining 1000 red blood cells. When 30 or more microgametocytes undergoing exflagellation were observed, the exflagellation-blocking assay was initiated [50].

Exflagellation-blocking bioassay

The exflagellation-blocking bioassays were carried out according to the protocol published by Delves et al. [14] with modifications. Gametocytes (stages IV, V) confirmed to undergo exflagellation were treated with DMSO (≤ 0.5%) as negative control. Dihydroartemisinin (DHA) at a final concentration of 1 µM was used as inhibitory control.

Bi-triazole compounds were tested at a concentration of 1 µM in triplicate. For the assay, 20 µL of the compounds or the reference drug were added to 180 µL of gametocyte culture in a 96-well plate (KASVI). The plate was incubated for 48 h, after which exflagellation was induced as described previously.

Compounds with inhibition ≥ 75% exflagellation at 1 µM concentration were selected as possibly active molecules in the exflagellation-blocking bioassay, which can be considered as having high likelihood to block malaria transmission. Compounds with mean exflagellation inhibition between 25 and 75% may have average likelihood of being active in blocking transmission; and compounds with exflagellation inhibition below 25% are considered inactive compounds in exflagellation inhibition and, consequently, in blocking transmission [51].

The percentage of exflagellation inhibition (EI) was calculated using the formula:

$$EI = \frac{Ec - Et * 100}{Ec}$$

EI = exflagellation inhibition; E_C = exflagellation of control; E_t = exflagellation with the test compound [51].

Data analysis

The raw data from each experiment were initially tabulated using Excel 2010. Dose–response curves of IC_{50} and CC_{50} were generated using Origin® 9.1 (OriginLab Corporation, Northampton, MA, USA). The values were calculated based non-linear regression, with statistical significance set at $p \leq 0.05$ and $R^2 \geq 0.95$.

Statistical difference in haemolysis values were analysed using GraphPad Prism v0.8.0 with Tukey's post-hoc test applied. For the exflagellation assays, statistical analyses were also performed using GraphPad Prism v0.8.0. Differences in microgametocytes inhibition results were evaluated using the Mann–Whitney test.

Results

In silico theoretical prediction of the compounds

To identify compounds with optimal physicochemical, pharmacokinetic, and toxicologic properties, in silico

screening was carried out for all compounds evaluated in this study.

None of the compounds exhibited positive drug-likeness values, which means no compound has fragments similar to those found in commercially available drugs [52]. For drug score values, none of the compounds achieved scores close to or exceeding 1. The toxicity prediction showed that none of the compounds in either chemical class exhibited warnings for mutagenicity, genotoxicity, or irritating. Compound 14c was classified as having moderate lipophilicity (cLogP), reflecting a balance between permeability and solubility. Compounds 14d, 13c, and 13d were classified as having low lipid bilayer permeability.

The results of the aqueous solubility prediction (LogS) showed that all compounds were classified as highly soluble in aqueous medium (Table 1). In this study, the evaluated compounds demonstrated slightly toxic to non-toxic properties, while meeting the criteria established by Lipinski [22] and Veber [23]. These criteria consider that pharmaceuticals with good oral bioavailability must have logP ≤ 5, molecular mass ≤ 500 g/mol, hydrogen bond acceptors ≤ 10, hydrogen bond donors ≤ 5, topological polar surface area (TPSA) ≤ 140 $Å^2$ and rotational bonds ≤ 10 (Table 2).

The pharmacokinetic parameters of the compounds were predicted using ADMETlab. This platform enabled calculating some parameters related to absorption, distribution, elimination, and toxicity. For absorption, the permeability results of Caco-2 cells predicted low permeability for all compounds (Table 3). Only 14c was identified as a P-flycoprotein (Pgp) inhibitor, none of the other compounds exhibited this action.

For distribution, three parameters were assessed: plasma protein binding (PPB), volume of distribution (Vd), and brain-blood barrier (BBB). All compounds exhibited low PPB, with specific values: 14c at 38.3%, 14d at 29.7%, 13c at 25.9%, and 13d at 38.4% (Table 3). In silico result for Vd yielded 0.04 L/kg, i.e., all compounds in this study are poorly distributed, as suggested by the following values: for 14c Vd = − 0.51 L/kg; for 14d, Vd = − 0.61 L/kg; for 13c, Vd = − 0.45 L/kg; and for 13d, Vd = − 0.61 L/kg (Table 3).

All compounds exhibited a high likelihood of crossing the blood–brain barrier and all exhibited negative status in the prediction to be a substrate for Pgp. Only compound 14c was shown to act as an inhibitor of the Pgp substrate (Table 3).

In addition to the predictions presented, another interesting characteristic in finding new pharmaceuticals is carrying out an in silico test to eliminate drugs. Therefore, the half-life of each compound was predicted and the results showed that all compounds had half-life under 2 h, which classifies them as having a short half-life (Table 3). Along with the half-life, the clearance rate (CL) was predicted, with all compounds being classified as having a low clearance rate.

Table 1 Osiris calculations on physicochemical properties and toxicity prediction of compounds 14c, 14d, 13c and 13d

Compounds	MW	Toxicity alert				Drug-score solubility			
		MUT	TUM	IRR	REP	DL	DS	cLogP	cLogS
14c	276.17	NT	NT	NT	MT	− 16.42	0.39	0.460	1.54
14d	276.17	NT	NT	NT	MT	− 13.5	0.39	− 0.015	1.69
13c	222.09	NT	NT	NT	MT	− 4.42	0.40	− 0.611	1.97
13d	222.09	NT	NT	NT	MT	− 1.49	0.46	− 0.015	2.12

MW molecular weight, *MUT* mutagenic, *TUM* tumorigenic, *IRR* irritating, *REP* reproductive, *DL drug-likeness*, *DS drug-score*, *cLogP* lipid solubility, *cLogS* solubility, *NT* non toxic, *MT* mildly toxic, *T* toxic

Table 2 In silico prediction of the physical–chemical properties and possible biological activities of the compounds 14c, 14d, 13c and 13d

Physicochemical properties						
Compounds	PSA	HBA	HBD	VIO	ROT	VOL
14c	98.60	7	1	0	5	201.81
14d	98.60	7	1	0	5	201.81
13c	98.60	7	1	0	4	187.07
13d	98.60	7	1	0	4	187.07

PSA polar surface area, *HBA* hydrogen acceptors, *HBD* hydrogen donors, *VIO* number of violations, *ROT* rotatable link numbers, *VOL* Van der Waals volume

Table 3 Prediction of pharmacokinetic properties of compounds 14c, 14d, 13c and 13d

ADMET	14c	14d	13c	13d
Absorption				
Caco-2	– 4.47 (log P_{app})	– 4.44 (log P_{app})	– 4.49 (log P_{app})	– 4.48 (log P_{app})
Pgp-inhibitor	Positive	Negative	Negative	Negative
Pgp-substrate	Negative	Negative	Negative	Negative
Distribution				
PPB	Low	Low	Low	Low
Vd	Low	Low	Low	Low
BBB	Positive	Positive	Positive	Positive
Elimination				
Half-life time ($T_{1/2}$)	0.95 h	0.91 h	0.87 h	0.91 h
Clearance elimination (CL)	1.441 mL/min/kg	1.379 mL/min/kg	1.422 mL/min/kg	1.379 mL/min/kg
Acute toxicity				
hERG	Negative	Negative	Negative	Negative
LD_{50}	204 mg/kg	187 mg/kg	835 mg/kg	187 mg/kg
DILI	Positive	Positive	Positive	Positive
FDAMDD	Positive	Positive	Positive	Positive

Caco-2 human epithelial cell line of the intestinal epithelial barrier, *Pgp* P-glycoprotein, *PPB* plasma protein binding, *Vd* volume of distribution, *BBB* blood brain barrier, Half-life time in hours, $T_{1/2}$, *hERG* human Ether-à-go-go-Related Gene, LD_{50}: 50% lethal dose, *DILI* Drug-induced liver injury, FDAMDD Maximum recommended daily dose

For acute oral toxicity, compounds 14c (LD_{50} = 204.33 mg/kg), 14d (LD_{50} = 187.58 mg/kg), and 13d (LD_{50} = 187.58 mg/kg) were classified as toxic and compound 13c (LD_{50} = 835.14 mg/kg) was classified as harmful (Table 3). In addition to the aforementioned toxicity parameters, all compounds were positive for DILI and FDAMDD, and negative for inhibition of the hERG channel (Table 3).

The metabolic activity of the compounds was evaluated by their potential to inhibit cytochrome P450 (CYP) enzymes. For enzyme CYP1A2, inhibition occurred only with compound 14c, whereas no compound was classified as inhibitory for enzymes CYP3A4, CYP2C9, CYP2D6, or CYP2C19.

Antiplasmodial and cytotoxic activity of the bi-triazole compounds

The IC_{50} values of the tested bi-triazole compounds varied for the *P. falciparum* W2 clone. Among the compounds (14c, 14d, 13c, and 13d), three of them (14c, 14d, and 13d) reached in vitro inhibition values below 25 µM. The respective IC_{50} values were 9.8 ± 0.4 µM for compound 14c, 3.1 ± 1.3 µM for compound 14d, 130.3 ± 7.6 µM for compound 13c, and 4.4 ± 0.2 µM for compound 13d (Table 4).

Regarding cytotoxicity, all compounds maintained cell viability rates above 80% when the cells were treated with the bi-triazoles at the highest concentration of 500 µM; all values were significant about the treatment with DMSO. In this sense, the mean viability rate of 84.3% was obtained for compound 14c, 93.4% for 14d, 89.9% for 13c, and 80% for 13d (Table 4).

Based on these findings, compounds 14c, 14d, and 13d were considered selective for the parasite and non-cytotoxic to HepG2 cells, exhibiting SI values above 51. In contrast, compound 13c was non-selective in light of its SI value (≥ 3) (Table 4).

Table 4 In vitro antimalarial activity against *P. falciparum* (W2 strain), cytotoxicity (HepG2 cells) and selectivity index of bi-triazole compounds

Bi-triazole	IC_{50} (µM) W2	CC_{50} (µM) HepG2	SI	Viability of HepG2 cells at 500 µM (%)
14c	9.8 ± 0.4	≥ 500	≥ 51	84.3
14d	3.1 ± 0.8	≥ 500	≥ 161	93.4
13c	130 ± 7.6	≥ 500	≥ 3	89.9
13d	4.4 ± 0.2	≥ 500	≥ 113	80
Artemisinin	0.021 ± 0.004	≥ 500	≥ 23,809	100

The table represents IC_{50} and CC_{50} values represented by the mean of three independent experiments; (±) standard deviation. Selectivity Index (SI). IC_{50}: 50% inhibitory concentration, defined as the concentration that inhibits 50% of the parasite growth in relation to control cultures with no drugs. CC_{50}: concentration that kills 50% of HepG2 cells, 72 h after incubation with the compounds determined by the MTT method

A haemolysis assay revealed that all tested compounds presented low haemolytic activity (3%), with no statistical difference from the negative control (untreated red blood cells). In contrast, the positive control (0.05% saponin) caused 100% haemolysis, showing a significant difference ($p \leq 0.05$).

In parallel with the tests against asexual forms, an exflagellation inhibition test was carried out aiming at determining the malaria-blocking potential of the compounds. The results showed that the most promising values were attributed to compounds 14c and 14d, inhibiting over 75% of exflagellating forms. Compound 13c did not show significant inhibition. Due to limited sample availability, compound 13d was not tested at this stage (Fig. 2).

Discussion

The need for novel antimalarial compounds with quick action, low cost, high selectivity, and acceptable physicochemical, pharmacokinetic, and toxicologic properties is critical. Beyond these characteristics, it is desirable for compounds to act against multiple stages or forms of the parasite [53]. Within this framework, triazole derivatives stand out to their broad range of diversified and well-discussed pharmacological properties [54].

Triazole derivatives are widely used worldwide. Various biological activities of drugs containing the triazole group in their structure have been reported, including antihypertensive [55] antiviral [56], antitumour [57], antifungal [56], antimicrobial [58], antiplasmodial [59, 60], among others.

The present study assessed the antiplasmodial activity of four bi-triazole compounds: 14c, 14d, 13c, and 13d. An analysis of their structure–activity relationship, suggests that specific substituents are crucial for plasmodial inhibition. For instance, substituent R_2 in all four compounds is represented by an ester group, differing only in the position of atoms (14d and 13d-methyl acetate substituent; 14c and 13c-ethyl carboxylate substituent) [17]. Based on this observation, it can be inferred that the antiplasmodial activity may be related to the presence of the methyl acetate substituent (CH_2COOCH_3) present in the R_2 of compounds 14d (IC_{50} 3.1 µM) and 13d (IC_{50} 4.4 µM) since the R_1 of the compounds is different. This hypothesis is further supported by comparing the antimalarial activity of compounds 13c (IC_{50} 130.3 µM), which contains a methyl substituent (-CH3) in R_1 and an ethyl carboxylate group in R_2, and compound 14c (IC_{50} 4.4 µM), which differs by having a methyl acetate group (CH_2COOCH_3) in R_2. The latter is 29 times more active against *P. falciparum* W2.

Compound 14d with an IC_{50} of 3.1 ± 1.3 µM, contains a trifluoromethyl group (-CF_3) in R_1 and a methyl acetate group in R_2. It exhibited greater activity than compound

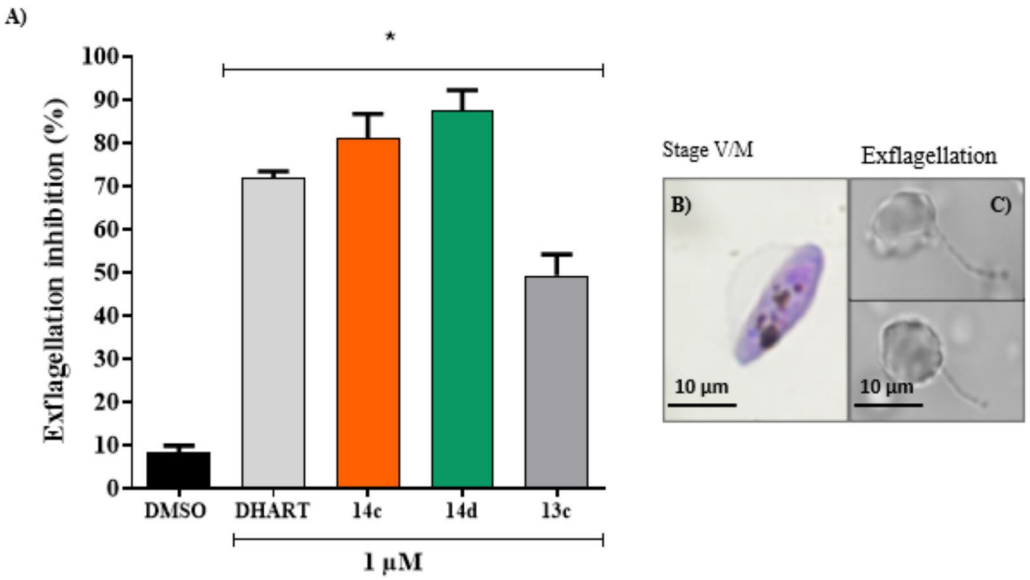

Fig. 2 *Plasmodium falciparum* exflagellation assay. **A** Exflagellation inhibition by compounds 14c, 14d, 13c, DMSO-negative control and DHART-positive control). **B** Image of mature stage V microgametocyte (Stage V/M). **C** Two different microgametocytes undergoing exflagellation. DMSO (Dimethylsulfoxide, negative control, C^-) ≤ 0.5%; DHART (Dihydroartemisinin, inhibitory control) at 1 µM and Bi-triazole compounds at 1 µM incubated for 24 h. Percent inhibition was calculated relative to the DMSO control. Data are presented as the mean and standard deviation (±) of duplicates from a single experiment. Statistical significance was analyzed using the Mann–Whitney test. Columns marked with an asterisk * indicate a statistically significant difference compared to the DMSO control ($p \leq 0.02$)

14c, which also has a similar structure (R_1 with -CF_3), with the difference in the (R_2) ethyl carboxylate substituent (-$COOCH_2CH_3$), with IC_{50} of 9.8 ± 0.4 µM. Thus, it can be inferred that the bi-triazole containing the trifluoromethyl substituent may have its inhibitory action potentiated against *P. falciparum* W2 when associated with group (R_2) methyl acetate (Table 4).

Fluorinated molecules, particularly those with trifluoromethyl groups, have shown as promising antimalarial candidates due to their favorable physicochemical properties (high electron affinity and lipophilicity) and pharmacokinetic (prolonged half-life and bioavailability) [61]. Similarly, acetylated groups enhance parasite inhibition by stabilizing hydrogen bonds, increasing lipophilicity, and improving resistance to breakdown, while maintaining low toxicity in HepG2 cells [62, 63].

When analysing the structure–activity relationship of the bi-triazole nucleus with its substituent, the data from this study reveal that the pharmacophoric group containing the ethyl carboxylate substituent in R_2 remains promising when associated with the trifluoromethyl substituent (-CF_3) R_1 with, as observed in compound 14c (IC_{50} = 9.8 µM; 14c). However, it can be decreased when associated with R_1 methyl substituent (-CH_3), as seen in compound 13c, whose IC_{50} value was above 25 µM (IC_{50} 130.3 ± 7.6 µM). According to the classification by Cos et al. [40], molecules are considered potentially active if they exhibit IC_{50} values ≤ 25 µM.

Comparing the two molecules with the best inhibition values (14d and 13d), both share the methyl acetate substituent I R_2, suggesting that this chemical group may contribute to antiplasmodial activity. Regarding toxicity, bi-triazoles 14c, 14d, and 13d demonstrated satisfactory IC_{50} values and exhibited no cytotoxicity at the highest concentration tested (500 µM). This combination of data resulted in promising SI values above 10, specifically 14c (SI ≥ 51), 14d (SI ≥ 98), and 13d (SI ≥ 113). On the other hand, compound 13c had and SI ≥ 3, indicating it was not selective for the parasite. According to the literature, compounds are considered safe if their SI values exceed 10, while values below 10 indicate high toxicty and non-selectivity [44–46]. As for the haemolytic percentage, it was observed that all compounds tested did not cause extensive damage to human cells.

To evaluate their potential to block malaria transmission, compounds were tested for their ability to inhibit microgametocyte exflagellation. Compounds 14d (87.3%) and 14c (81.0%) at 1 µM showed strong potential to block malaria transmission. Compound 13c exhibited moderate inhibition (49.3%). Microgametocytes are known to be more susceptible to antimalarials than macrogametocytes suggesting the need for future studies targeting female gametocyte forms [14].

The findings suggest that new synthesis strategies could focus on maintaining bi-triazole pharmacophoric nucleus while incorporating substituents to enhance antimalarial activity. Adding a methyl group (-CH_3) may increase lipophilic, hydrophobic interactions, and, some cases, solubility, though it may also reduce bioavailability or hinder target interaction [61].

However, some studies also state that introducing methyl into a molecule may cause an increase in lipophilicity, which might change the bioavailability of the molecule, making it inactive or even hindering its interaction with its possible target [62]. In the context of this study, that chemical group did not favor the antiplasmodial activity of bi-triazole when it had in its R_2 the ethyl carboxylate group in compound 13c (IC_{50} 130.3 µM). Nonetheless, introducing the methyl group in R_1 of the bi-triazole nucleus and the methyl acetate group in its R_2 (13d) led to activity below 10 µM at 72 h. Such results show that the same substituent defines different molecule parameters and potency, even with small alterations in them.

The fluoride atom (F), present in compounds 14c and 14d (IC_{50} ≤ 10 µM), is widely employed in medicinal chemistry for its ability to enhance bioactive compound properties. It provides chemical, metabolic, conformational, and lipophilic stability, prevents oxidation, and adjusts basicity, addressing drug metabolism challenges [64, 65].

Another interesting characteristic is the C-F bond is notably more stable and resistant to metabolic oxidation compared to the C-H bond, providing to greater lipophilicity [66]. Fluoride's high electronegativity also strongly influences the acidity or alkalinity of nearby functional groups, enhancing bioavailability and membrane permeation [67]. Notable antimalarials featuring the trifluoromethyl group include mefloquine, halofantrine and tafenoquine [68].

The ester groups in R_2 across all studied compounds contribute to diverse parameters, such as size, shape, charge distribution, lipophilicity, all of which are crucial for pharmacokinetic improvements (a.g., absorption and distribution) and molecular stability [63].

The lipophilicity found in compound 14c (featuring fluoride and ethyl carboxylate-ester) is higher than in compound 13c (with methyl and ethyl carboxylate-ester), potentially enhancing its interaction with host cells and increasing its antiplasmodial efficacy.

The combination of a methyl substituent (-CH_3) and methyl acetate ester (CH_2COOCH_3) in 13d significantly enhances antiplasmodial activity. Although substituents play a critical hole, the bi-triazole nucleus itself in triggering pharmacological action, as evidenced in this study.

Theoretical in silico assessments of physicochemical and ADME (absorption, administration, distribution, metabolism, and excretion) properties revealed promising toxicity profiles for all compounds. Results for mutagenicity, tumorigenicity, reproductive toxicity, and irritating indicated non-toxic to slightly toxic classifications, confirming that those compounds possibly lack toxicity for either chemical class. All compounds met physicochemical criteria [22, 23], improving their prospects for drug development.

However, none of the compounds showed positive drug-likeness values or drug score near 1, indicating a lack of similarity to existing drugs [52]. Nonetheless, this does not preclude their classification as future candidates for malaria or other diseases.

Regarding membrane permeability and distribution, only compound 14c achieved a balance between permeability and solubility, classifying it as a potential candidate for oral pharmaceuticals [24] due its substituents R_1 (trifluoromethyl) and R_2 (ethyl carboxylate) substituents. Other compounds fell short of this threshold, potentially limiting their oral bioavailability [24].

Using Caco-2 cells for in silico intestinal permeability predictions [69, 70], most compounds displayed low solubility, likely due to their solubility in aqueous medium. Compound 14c stood out, exhibiting balanced permeability and solubility. The volume of distribution (Vd), which measures drug distribution within the body, was low for all compounds (optimal range: 0.04–20 L/kg), possibly due to hydrophilic properties or low binding to plasma proteins.

Clearance refers to the rate at which compounds are eliminated, typically by kidneys, liver, or bile [29, 32]. Faster clearance shortens half-life, especially when paired with a small Vd [71]. According to Di and Obach [72], drugs with low clearance may require smaller doses, enhancing exposure and extending half-life. However, prolonged half-lives can increase side effects due to extended drug presence. In the context of malaria treatment, tafenoquine was recently approved for the radical cure of *P. vivax* in a single-dose regimen, promoting greater patient adherence to treatment. However, like primaquine, tafenoquine can cause haemolysis in G6PD-deficient individuals [73].

In this study, none of the compounds showed a high affinity for binding to blood plasma proteins; all were classified as low-affinity binders [29, 67]. Compounds with low plasma protein binding, such as bi-triazoles, can be more widely distributed, as only the free drug is available for tissue distribution [74]. Unbound drugs are also more rapidly exposed to enzymes and targets, enhancing their pharmacological effect [75]. However, they may be eliminated faster, as only the free form is excreted by the kidneys [76]. For antimalarials, in silico predictions revealed that commonly used malaria drugs, such as artemisinin, chloroquine, primaquine, and mefloquine, exhibit high plasm protein binding [77]. This often prolongs half-life and slows clearance, though artemisinin and its derivatives are exceptions [78].

P-glycoprotein (Pgp), expressed in organs such as the intestinal epithelium, pancreatic and bile ducts, renal tubules, and brain capillaries, plays a key role in preventing toxin entry into cells. Pgp functions as both a barrier and a secretion mechanism [79], aiding in the removal of foreign substances [80]. It recognizes a wide range of compounds (300–4,000 molecular weight), impacting bioavailability, toxicity, and metabolism [80, 81].

Pgp tends to recognize hydrophobic drugs, which can lead to therapeutic failure [82]. In this study, only compound 14c was identified as a Pgp inhibitor, suggesting potential bioavailability challenges, unlike the other compounds, which did not inhibit Pgp. P-glycoproteins share many substrates with the enzyme CYP3A4, which is involved in the transport of drugs from various chemical classes [83]. Another crucial factor in drug development is the blood–brain barrier (BBB), a selective permeability barrier that maintains CNS homeostasis. Despite medical advances, CNS- related diseases remain prevalent and often lack effective treatments [84]. In this study, all compounds showed the ability to cross the BBB in silico, suggesting their potential for developing drugs targeting cerebral malaria. This severe and often fatal, associated with *P. falciparum*, remains a significant challenge due to rising drug resistance and limited therapeutic options [85].

Drug-induced liver injury (DILI) refers to liver damage caused by pharmaceuticals. Although it is a critical parameter to assess, it is often overlooked, allowing such injuries to progress to liver failure [86]. The hepatotoxicity of drugs that cause DILI in humans is typically unclear in animal models and not always dose-dependent. Morover, DILI may occur in fewer than 1 in 10,000 to 100,000 individuals who take the drug [87]. In this study, in silico analysis suggested that all compounds might pose a risk for DILI, albeit with a low incidence rate. Thus, these compounds should be carefully monitored if considered for use in treating other diseases. The maximum recommended daily dose (FDAMDD) is a pharmacokinetic parameter tied to drug bioavailability, encompassing absorption, rate, half-life, and clearance. Compounds with rapid elimination and low distribution volumes would require administration at their maximum daily dosage, as observed for all FDAMDD-positive compounds in this study. As noted earlier, all compounds were classified as having short half-lives (i.e., under 2 h). To avoid dosing intervals shorter than 2 h, one potential

strategy could involve administering higher doses to extend the interval [88]. However, implementing this approach requires careful evaluation of pharmacokinetic parameters and toxicity profiles [89].

Some compounds in this study had LD_{50} values between 50 mg/kg and 300 mg/kg, indicating potential toxicity but not lethality. According to Macherey and Dansette [90], metabolic bioactivation is a common cause of toxicity. CYP enzymes, primarily located in the liver, play a central role in drug metabolism. The CYP families 3A (28%), 2D6 (21%), and 2C (18%) collectively metabolize approximately 90% of drugs. Other enzymes, such as 1A2 (13%), 2E1 (7%), and 2A6 (4%), contribute to a lesser extent [91]. In this study, all compounds except 14c showed no inhibition of cytochrome P450 enzymes. This lack of inhibition could negatively impact clinical biotransformation or elimination, leading to increased plasma concentrations of compound 14c, potentially affecting its therapeutic efficacy and raising the risk of adverse effects [92, 93].

Conclusion

The results represent the discovery of a potential chemical class for further exploration, not only for its antiplasmodial activity but also for other potential therapeutic applications. This potential is supported by in silico and in vitro safety findings (cytotoxicity and haemolysis). This study is one of the first to report gametocytocidal activity for bi-triazole compounds, particularly emphasizing the dual action of compound 14d, which targets parasites in both asexual and sexual stages (including microgametocytes) at concentrations below 3.1 μM. Additionally, substituent groups 1 and 2 were shown to play key roles in the antimalarial activity of this class of molecules. The bi-triazole core linked to substituents such as trifluoromethyl and methyl acetate, methyl and methyl acetate, or trifluoromethyl and ethyl carboxylate proved effective in inhibiting parasite growth, with IC_{50} values below 10 μM. Based on these results, compound 14d shows potential for development as a drug candidate targeting both asexual and sexual forms of malaria.

Acknowledgements
We thank Fiocruz Rondônia and the Platform for Infection of Vectors of Malaria (PIVEM/ Laboratório de Entomologia, Fundação Oswaldo Cruz, FIOCRUZ, unidade Rondônia) for all the support offered in the construction of this work.

Author contribution
Leandro do Nascimento Martinez: Conceptualization, Data curation, Formal analysis, Writing-original draft. Minelly Azevedo da Silva: Conceptualization, Investigation, Methodology. Saara Neri Fialho: Data curation. Marcinete Latorre Almeida: Data curation. Amália dos Santos Ferreira: Data curation. Aurileya de Jesus Gouveia: Data curation. Welington da Silva Paula do Nascimento: Data curation. Ana Paula de Azevedo dos Santos: Formal analysis, Writing-original draft. Norton Rubens Diunior Lucas Pejara Rossi: Formal analysis. Maisa da Silva Araújo: Conceptualization, Data curation, Formal analysis, Writing-original draft. Natalie Ferreira Araújo: Data curation. Quelli Larissa Oliveira de Santana: Data curation. Carlos Roland Kaiser: Data curation. Sabrina Baptista Ferreira: Data curation, Writing-review & editing, Visualization. Jansen Fernandes de Medeiros: Data curation. Carolina Bioni Garcia Teles: Data curation, Writing-review & editing, Visualization All authors approved the final version of the manuscript.

Funding
This work was supported, in part, by the Brazilian Ministry of Health/DECIT/CNPq N 23/2019 (grant number 442653/2019-0) and the Bill & Melinda Gates Foundation (INV-003970). Under the grant conditions of the foundation, a Creative Commons Attribution 4.0 Generic License has already been assigned to the author-accepted manuscript version that might arise from this submission. The authors express their gratitude to Conselho Nacional de Desenvolvimento Científico e Tecnológico (CNPq), Coordenação de Aperfeiçoamento de Pessoal de Nível Superior (CAPES), Programa Inovação na Amazônia (Fiocruz, Fapeam e FAPERO), Instituto Nacional de Ciência e Tecnologia, Epidemiologia da Amazônia Ocidental (INCT-EpiAmO), and the Fundação Oswaldo Cruz (Fiocruz) for the financial support.

Data availability
No datasets were generated or analysed during the current study.

Declarations

Ethics approval and consent to participate
The study was approved by the Ethics Committee for Research with Human Beings—(CEP)—CAAE: 56853922.2.0000.5300—UNIR.

Consent for publication
Not applicable.

Conflict of interest
The authors declare no competing interests.

Author details
[1]Plataforma de Bioensaios de Malária E Leishmaniose (PBML), Fundação Oswaldo Cruz, FIOCRUZ, Unidade Rondônia, Porto Velho, RO, Brazil. [2]Programa de Pós-Graduação Em Biologia Experimental (PGBIOEXP), Fundação Universidade Federal de Rondônia (UNIR), Porto Velho, RO, Brazil. [3]Centro Universitário São Lucas -PVH/Afya, Porto Velho, RO, Brazil. [4]Instituto Federal de Educação, Ciência e Tecnologia de Rondônia – IFRO, Porto Velho, Brazil. [5]Programa de Pós-Graduação em Biodiversidade e Biotecnologia da Amazônia Legal – BIONORTE, Porto Velho, RO, Brazil. [6]Plataforma de Infecção de Vetores da Malária (PIVEM/ Laboratório de Entomologia, Fundação Oswaldo Cruz, FIOCRUZ, UnidadeRondônia, Porto Velho, RO, Brazil. [7]LaSOPB – Laboratório de Síntese Orgânica e Prospecção Biológica, InstitutodeQuímica, Universidade Federal Do Rio de Janeiro, Rio de Janeiro, RJ 21941-909, Brazil. [8]Instituto Nacional de Epidemiologia da Amazônia Ocidental – EpiAmO, Porto Velho, RO, Brazil.

Received: 11 July 2024 Accepted: 15 February 2025
Published online: 04 March 2025

References

1. WHO. World malaria report 2023 Geneva, World Health Organization, 2023. https://www.who.int/teams/global-malaria-programme/reports/world-malaria-report-2023. Accessed 16 Nov 2024.
2. Khoury DS, Cao P, Zaloumis SG, Davenport MP. Artemisinin resistance and the unique selection pressure of a short-acting antimalarial. Trends Parasitol. 2020;36:884–7.
3. Ferreira MU, Nobrega de Sousa T, Rangel GW, Johansen IC, Corder RM, Ladeia-Andrade S, et al. Monitoring *Plasmodium vivax* resistance to antimalarials: persisting challenges and future directions. Int J Parasitol Drugs Drug Resist. 2021;15:9–24.
4. Noedl H, Se Y, Schaecher K, Smith BL, Socheat D, Fukuda MM. Evidence of artemisinin-resistant malaria in western Cambodia. N Engl J Med. 2008;359:2619–20.

5. Poonam, Gupta Y, Gupta N, Singh S, Wu L, Chhikara BS, et al. Multistage inhibitors of the malaria parasite: emerging hope for chemoprotection and malaria eradication. Med Res Rev. 2018;38:1511–35.
6. Tran TM, Crompton PD. Decoding the complexities of human malaria through systems immunology. Immunol Rev. 2020;293:144–62.
7. Delves MJ, Miguel-Blanco C, Matthews H, Molina I, Ruecker A, Yahiya S, et al. A high throughput screen for next-generation leads targeting malaria parasite transmission. Nat Commun. 2018;9:3805.
8. Tilley L, Straimer J, Gnädig NF, Ralph SA, Fidock DA. Artemisinin action and resistance in *Plasmodium falciparum*. Trends Parasitol. 2016;32:682–96.
9. Munro BA, McMorran BJ. Antimalarial drug strategies to target *Plasmodium* gametocytes. Parasitologia. 2022;2:101–24.
10. Rodrigo C, Rajapakse S, Fernando SD. Primaquine and tafenoquine for preventing malaria in people travelling to or living in endemic areas. Cochrane Database Syst Rev. 2019;2019:CD012242.
11. WHO. World malaria report—Policy brief on single-dose primaquine as a gametocytocide in *Plasmodium falciparum* malaria. [Internet]. Geneva, World Health Organization, 2015. https://cdn.who.int/media/docs/default-source/documents/publications/gmp/policy-brief-on-single-dose-primaquine-as-a-gametocytocide-in-plasmodium-falciparum-malaria.pdf?sfvrsn=cab14722_2. Accessed 8 Jan 2025.
12. WHO. World malaria report 2024. Geneva, World Health Organization, 2024. https://iris.who.int/bitstream/handle/10665/379635/B09146-eng.pdf?sequence=1. Accessed 8 Jan 2025.
13. Looareesuwan P, Krudsood S, Lawpoolsri S, Tangpukdee N, Matsee W, Nguitragool W, et al. Gametocyte prevalence and risk factors of *P. falciparum* malaria patients admitted at the hospital for tropical diseases, Thailand: a 20-year retrospective study. Malar J. 2023;22:321.
14. Delves MJ, Ruecker A, Straschil U, Lelièvre J, Marques S, López-Barragán MJ, et al. Male and female *Plasmodium falciparum* mature gametocytes show different responses to antimalarial drugs. Antimicrob Agents Chemother. 2013;57:3268–74.
15. Xia Y, Fan Z, Yao J, Liao Q, Li W, Qu F, et al. Discovery of bitriazolyl compounds as novel antiviral candidates for combating the tobacco mosaic virus. Bioorg Med Chem Lett. 2006;16:2693–8.
16. Demirci S, Basoglu S, Bozdereci A, Demirbas N. Preparation and antimicrobial activity evaluation of some new bi- and triheterocyclic azoles. Med Chem Res. 2013;22:4930–45.
17. Addla D, Diniz C, de Larissa Oliveira Santana Q, Do Nascimento Martinez L, Latorre Almeida M, Azevedo Da Silva M, et al. Synthesis of new bi-triazoles with plasmocide action against *Plasmodium falciparum*. Curr Bioact Compd. 2023;19:18–28.
18. Lombardo F, Desai PV, Arimoto R, Desino KE, Fischer H, Keefer CE, et al. In silico absorption, distribution, metabolism, excretion, and pharmacokinetics (ADME-PK): utility and best practices. An industry perspective from the international consortium for innovation through quality in pharmaceutical development. J Med Chem. 2017;60:9097–113.
19. Miguel-Blanco C, Molina I, Bardera AI, Díaz B, de las Heras L, Lozano S, et al. Hundreds of dual-stage antimalarial molecules discovered by a functional gametocyte screen. Nat Commun. 2017;8:15160.
20. Ioset J-R, Brun R, Wenzler T, Kaiser M, Yardley V. Drug screening for kinetoplastids diseases: a training manual for screening in neglected diseases. DNDi and Pan-Asian Screening Network. 2009. https://dndi.org/scientific-articles/2009/drug-screening-for-kinetoplastid-diseases-a-training-manual-for-screening-in-neglected-diseases/. Accessed 16 Nov 2024.
21. Daina A, Michielin O, Zoete V. SwissADME: a free web tool to evaluate pharmacokinetics, drug-likeness and medicinal chemistry friendliness of small molecules. Sci Rep. 2017;7:42717.
22. Lipinski CA. Lead- and drug-like compounds: the rule-of-five revolution. Drug Discov Today Technol. 2004;1:337–41.
23. Veber DF, Johnson SR, Cheng HY, Smith BR, Ward KW, Kopple KD. Molecular properties that influence the oral bioavailability of drug candidates. J Med Chem. 2002;45:2615–23.
24. Kerns EH, Di L. Lipophilicity. In: Drug-like properties: concepts, structure design and methods. 1st ed. San Diego: Elsevier; 2008.
25. Pham The H, González-Álvarez I, Bermejo M, Mangas Sanjuan V, Centelles I, Garrigues TM, et al. In silico prediction of Caco-2 cell permeability by a classification QSAR approach. Mol Inform. 2011;30:376–85.
26. Chen L, Li Y, Zhao Q, Peng H, Hou T. ADME evaluation in drug discovery. 10. Predictions of P-glycoprotein inhibitors using recursive partitioning and naive bayesian classification techniques. Mol Pharm. 2011;8:889–900.
27. Poongavanam V, Haider N, Ecker GF. Fingerprint-based in silico models for the prediction of P-glycoprotein substrates and inhibitors. Bioorg Med Chem. 2012;20:5388–95.
28. Kumar R, Sharma A, Siddiqui MH, Tiwari RK. Prediction of drug-plasma protein binding using artificial intelligence based algorithms. Comb Chem High Throughput Screen. 2018;21:57–64.
29. Belpaire FM, Bogaert MG. The fate of xenobiotics in living organisms. In: Wermuth C, editor. The practice of medicinal chemistry. 2nd ed. Amsterdam: Elsevier Inc; 2003.
30. Li H, Yap CW, Ung CY, Xue Y, Cao ZW, Chen YZ. Effect of selection of molecular descriptors on the prediction of blood–brain barrier penetrating and nonpenetrating agents by statistical learning methods. J Chem Inf Model. 2005;45:1376–84.
31. Sanguinetti MC, Mitcheson JS. Predicting drug–hERG channel interactions that cause acquired long QT syndrome. Trends Pharmacol Sci. 2005;26:119–24.
32. Kerns EH, Di L. Pharmacokinetics. In: Drug-like properties: concepts, structure design and methods. 1st ed. San Diego: Elsevier; 2008. p. 228–41.
33. GHS. Globally Harmonized System of Classification and Labelling of Chemicals (GHS). 2023; p. 1–592. https://unece.org/sites/default/files/2023-07/GHS%20Rev10e.pdf. Accessed 16 Nov 2024.
34. Xu Y, Dai Z, Chen F, Gao S, Pei J, Lai L. deep learning for drug-induced liver injury. J Chem Inf Model. 2015;55:2085–93.
35. Cao D-S, Zhao J-C, Yang Y-N, Zhao C-X, Yan J, Liu S, et al. In silico toxicity prediction by support vector machine and SMILES representation-based string kernel. SAR QSAR Environ Res. 2012;23:141–53.
36. Trager W, Jensen JB. Human malaria parasites in continuous culture. Science. 1976;193:673–5.
37. Lambros C, Vanderberg JP. Synchronization of *Plasmodium falciparum* erythrocytic stages in culture. J Parasitol. 1979;65:418.
38. Smilkstein M, Sriwilaijaroen N, Kelly JX, Wilairat P, Riscoe M. Simple and inexpensive fluorescence-based technique for high-throughput antimalarial drug screening. Antimicrob Agents Chemother. 2004;48:1803–6.
39. Bagavan A, Rahuman AA, Kaushik NK, Sahal D. In vitro antimalarial activity of medicinal plant extracts against *Plasmodium falciparum*. Parasitol Res. 2011;108:15–22.
40. Cos P, Vlietinck AJ, Berghe DV, Maes L. Anti-infective potential of natural products: how to develop a stronger in vitro 'proof-of-concept. J Ethnopharmacol. 2006;106:290–302.
41. Calvo-Calle JM, Moreno A, Eling WMC, Nardin EH. In vitro development of infectious liver stages of *P. yoelii* and *P. berghei* malaria in human cell lines. Exp Parasitol. 1994;79:362–73.
42. Mosmann T. Rapid colorimetric assay for cellular growth and survival: application to proliferation and cytotoxicity assays. J Immunol Methods. 1983;65:55–63.
43. Wang C, Qin X, Huang B, He F, Zeng C. Hemolysis of human erythrocytes induced by melamine–cyanurate complex. Biochem Biophys Res Commun. 2010;402:773–7.
44. Nogueira F, do Rosário VE. Methods for assessment of antimalarial activity in the different phases of the *Plasmodium* life cycle. Rev Panamazonica Saude. 2010;1:109–24.
45. Gomes PR, Miguel FB, de Oliveira MÉ, Ferreira VV, Guimarães DSM, de Lima AB, et al. Synthesis and evaluation of antimalarial activity of curcumin derivatives. Quim Nova. 2014;37:492–6.
46. Katsuno K, Burrows JN, Duncan K, van Huijsduijnen RH, Kaneko T, Kita K, et al. Hit and lead criteria in drug discovery for infectious diseases of the developing world. Nat Rev Drug Discov. 2015;14:751–8.
47. Delves MJ, Straschil U, Ruecker A, Miguel-Blanco C, Marques S, Dufour AC, et al. Routine in vitro culture of *P. falciparum* gametocytes to evaluate novel transmission-blocking interventions. Nat Protoc. 2016;11:1668–80.
48. Duffy S, Avery VM. Identification of inhibitors of *Plasmodium falciparum* gametocyte development. Malar J. 2013;12:408.
49. Miao J, Wang Z, Liu M, Parker D, Li X, Chen X, et al. *Plasmodium falciparum*: generation of pure gametocyte culture by heparin treatment. Exp Parasitol. 2013;135:541–5.
50. Leba L-J, Musset L, Pelleau S, Estevez Y, Birer C, Briolant S, et al. Use of *Plasmodium falciparum* culture-adapted field isolates for *in vitro* exflagellation-blocking assay. Malar J. 2015;14:234.

51. Colmenarejo G, Lozano S, González-Cortés C, Calvo D, Sanchez-Garcia J, Matilla J-LP, et al. Predicting transmission blocking potential of antimalarial compounds in the mosquito feeding assay using *Plasmodium falciparum* male gamete inhibition assay. Sci Rep. 2018;8:7764.
52. Magalhães U de O. Modelagem molecular e avaliação da relação estruturaatividade acoplados a estudos físico-químicos, farmacocinéticos e toxicológicos In silico de derivados heterocíclicos com atividade leishmanicida. Dissertation, Federal University of Rio de Janeiro. 2009. https://ddec1-0-en-ctp.trendmicro.com:443/wis/clicktime/v1/query?url=http%3a%2f%2fobjdig.ufrj.br%2f59%2fteses%2f725703.pdf&umid=6b3db0f3-d9e8-4a79-b434-6ada4b9219e7&auth=1bcda6227c1853a98db9a85322c3ec3db27ad845-84d8fdb12cf65ba1865f094d7086d073dc16c488. Accessed 16 Nov 2024.
53. Reader J, van der Watt ME, Taylor D, Le Manach C, Mittal N, Ottilie S, et al. Multistage and transmission-blocking targeted antimalarials discovered from the open-source MMV Pandemic Response Box. Nat Commun. 2021;12:269.
54. Dheer D, Singh V, Shankar R. Medicinal attributes of 1,2,3-triazoles: Current developments. Bioorg Chem. 2017;71:30–54.
55. Liu J, Liu Q, Yang X, Xu S, Zhang H, Bai R, et al. Design, synthesis, and biological evaluation of 1,2,4-triazole bearing 5-substituted biphenyl-2-sulfonamide derivatives as potential antihypertensive candidates. Bioorg Med Chem. 2013;21:7742–51.
56. Hamim H, Sangeda RZ, Bundala M, Mkumbwa S, Bitegeko A, Sillo HB, et al. Utilization trends of antiviral and antifungal agents for human systemic use in Tanzania from 2010 to 2017 using the World Health Organization Collaborating Centre for Drug Statistics Methodology. Front Trop Dis. 2021;2:723991.
57. Ibba R, Piras S, Corona P, Riu F, Loddo R, Delogu I, et al. Synthesis, antitumor and antiviral in vitro activities of new benzotriazole-dicarboxamide derivatives. Front Chem. 2021;9:660424.
58. Goodman LS, Gilman AG. Goodman and Gilman's: pharmacological basis of therapeutics. 8th ed. New York: Mcgraw-Hill; 1991.
59. Oramas-Royo S, López-Rojas P, Amesty A, Gutiérrez D, Flores N, Martín-Rodríguez P, et al. Synthesis and antiplasmodial activity of 1,2,3-triazole-naphthoquinone conjugates. Molecules. 2019;2019(24):3917.
60. Costa Souza RM, Montenegro Pimentel LML, Ferreira LKM, Pereira VRA, Santos ACDS, Dantas WM, et al. Biological activity of 1,2,3-triazole-2-amino-1,4-naphthoquinone derivatives and their evaluation as therapeutic strategy for malaria control. Eur J Med Chem. 2023;255:115400.
61. Bazzini P, Wermuth CG. Substituent groups. In: Wermuth CG, Aldous D, Raboisson P, Rognan D, editors. The practice of medicinal chemistry. 4th ed. San Diego: Elsevier; 2008. p. 319–57.
62. Barreiro EJ, Kümmerle AE, Fraga CAM. The methylation effect in medicinal chemistry. Chem Rev. 2011;111:5215–46.
63. Ballatore C, Huryn DM, Smith AB. Carboxylic acid (Bio)isosteres in drug design. ChemMedChem. 2013;8:385–95.
64. Gillis EP, Eastman KJ, Hill MD, Donnelly DJ, Meanwell NA. Applications of fluorine in medicinal chemistry. J Med Chem. 2015;58:8315–59.
65. Böhm H-J, Banner D, Bendels S, Kansy M, Kuhn B, Müller K, et al. Fluorine in medicinal chemistry. ChemBioChem. 2004;5:637–43.
66. Park BK, Kitteringham NR, O'Neill PM. Metabolism of fluorine-containing drugs. Annu Rev Pharmacol Toxicol. 2001;41:443–70.
67. Kerns EH, Di L. Plasma protein binding. In: Drug-like properties: concepts, structure design and methods. 1st ed. San Diego: Elsevier; 2008. p. 187–96.
68. Tse EG, Korsik M, Todd MH. The past, present and future of anti-malarial medicines. Malar J. 2019;18:93.
69. Hosey CM, Benet LZ. Predicting the extent of metabolism using *in vitro* permeability rate measurements and in silico permeability rate predictions. Mol Pharm. 2015;12:1456–66.
70. Yee S. *In vitro* permeability across Caco-2 cells (colonic) can predict *in vivo* (small intestinal) absorption in man—Factor or myth. Pharm Res. 1997;14:4.
71. Roberts F, Freshwater-Turner D. Pharmacokinetics and anaesthesia. Continuing Educ Anaesth Crit Care Pain. 2007;7:25–9.
72. Di L, Obach RS. Addressing the challenges of low clearance in drug research. AAPS J. 2015;17:352–7.
73. Commons RJ, McCarthy JS, Price RN. Tafenoquine for the radical cure and prevention of malaria: the importance of testing for G6PD deficiency. Med J Aust. 2020;212:152.
74. Øie S, Tozer TN. Effect of altered plasma protein binding on apparent volume of distribution. J Pharm Sci. 1979;68:1203–5.
75. Sun L, Yang H, Li J, Wang T, Li W, Liu G, et al. In silico prediction of compounds binding to human plasma proteins by QSAR models. ChemMedChem. 2018;13:572–81.
76. Levy G. Effect of plasma protein binding on renal clearance of drugs. J Pharm Sci. 1980;69:482–3.
77. Pornputtapong N, Suriyapakorn B, Satayamapakorn A, Larpadisorn K, Janviriyakul P, Khemawoot P. In silico analysis for factors affecting antimalarial penetration into red blood cells. Malar J. 2020;19:215.
78. Benakis A, Paris M, Loutan L, Plessas CT, Plessas ST. Pharmacokinetics of artemisinin and artesunate after oral administration in healthy volunteers. Am J Trop Med Hyg. 1997;56:17–23.
79. Sharom FJ. ABC multidrug transporters: structure, function and role in chemoresistance. Pharmacogenomics. 2008;9:105–27.
80. Zhou S-F. Structure, function and regulation of P-glycoprotein and its clinical relevance in drug disposition. Xenobiotica. 2008;38:802–32.
81. Huber PC, Maruiama CH, Almeida WP. Glicoproteína-P, resistência a múltiplas drogas (MDR) e relação estrutura-atividade de moduladores. Quim Nova. 2010;33:2148–54.
82. Borst P, Evers R, Kool M, Wijnholds J. A family of drug transporters: the multidrug resistance-associated proteins. J Natl Cancer Inst. 2000;92:1295–302.
83. Finch A, Pillans P. P-glycoprotein and its role in drug-drug interactions. Aust Prescr. 2014;37:137–9.
84. Miao R, Xia L-Y, Chen H-H, Huang H-H, Liang Y. Improved classification of blood-brain-barrier drugs using deep learning. Sci Rep. 2019;9:8802.
85. Nishanth G, Schlüter D. Blood–brain barrier in cerebral malaria: pathogenesis and therapeutic intervention. Trends Parasitol. 2019;35:516–28.
86. Suh JI. Drug-induced liver injury. Yeungnam Univ J Med. 2020;37:2–12.
87. Chalasani N, Fontana RJ, Bonkovsky HL, Watkins PB, Davern T, Serrano J, et al. Causes, clinical features, and outcomes from a prospective study of drug-induced liver injury in the United States. Gastroenterology. 2008;135:1924–34.
88. Sahin S, Benet LZ. The operational multiple dosing half-life: a key to defining drug accumulation in patients and to designing extended release dosage forms. Pharm Res. 2008;25:2869–77.
89. Smith DA, Beaumont K, Maurer TS, Di L. Relevance of half-life in drug design. J Med Chem. 2018;61:4273–82.
90. Macherey AC, Dansette PM. Chemical mechanisms of toxicity: basic knowledge for designing safer drugs. In: The practice of medicinal chemistry. 2nd ed. Amsterdam: Elsevier; 2003. p. 545–60.
91. Kerns EH, Di L. Cytochrome P450 inhibition. In: Drug-like properties: concepts, structure design and methods San Diego. Amsterdam: Elsevier; 2008. p. 197–208.
92. Kalra B. Cytochrome P450 enzyme isoforms and their therapeutic implications: an update. Indian J Med Sci. 2007;61:102.
93. Kumar S, Sharma R, Roychowdhury A. Modulation of cytochrome-P450 inhibition (CYP) in drug discovery: a medicinal chemistry perspective. Curr Med Chem. 2012;19:3605–21.

Publisher's Note